REPORT R-425 AUGUST, 1969

CSL COORDINATED SCIENCE LABORATORY

TUNNELING IN SEMICONDUCTORS

C.B. DUKE

UNIVERSITY OF ILLINOIS - URBANA, ILLINOIS

TUNNELING IN SEMICONDUSTORS

C.B. Duke

Coordinated Science Laboratory and Department of Physics
University of Illinois
Urbana, Illinois

This work was supported in part by the Jet Propulsion Laboratory (National Aeronautics and Space Administration) under Contract No. JPL 952383; and in part by the Joint Services Electronics Program (U. S. Army, U. S. Navy, and U.S. Air Force) under Contract No. DAAB 07-67-C-0199.

TUNNELING IN SEMICONDUCTORS*

C. B. Duke

Coordinated Science Laboratory and Department of Physics
University of Illinois
Urbana, Illinois

ABSTRACT

Historical highlights of studies of current flow across metal-semiconductor contacts via electron tunneling are outlined. The physical origin of the space-charge potential at a rectifying metal contact on a degenerate semiconductor is illustrated with emphasis on the features of this potential which determine the dominant mechanism of current flow across the contact. Recent experiments on the tunneling characteristics of these junctions are described. Their interpretation in terms of phenomenological independent-electron models is discussed critically. The tunneling spectroscopy of collective excitations is described by use of the transfer-Hamiltonian model. The influence of features of the phonon spectra in the semiconductor on inelastic tunneling is illustrated for Ge. The effects of electronic interactions with collective excitations in the semiconductor electrode are discussed for phonons in Si and CdS, and for plasmons in GaAs. The references given herein supplement those presented in a recent comprehensive review.

* Supported in part by the Jet Propulsion Laboratory (National Aeronautics and Space Administration) under Contract No. JPL 952383, and by the Joint Services Electronics Program, U. S. Army Contract DAAB-07-67-C-0199.

TUNNELING IN SEMICONDUCTORS

The invention of the p-n tunnel diode by Esaki[1] in 1957 provided the first definitive experimental observation of tunneling as a mechanism of current flow in a junction between two solid electrodes. The development of one-electron models of tunneling from metals into semiconductors[2-5] and of interband tunneling in semiconductors[6] occurred in the early years of quantum theory. However, it was the subsequent development of the materials technology of semiconductors which permitted the first observations of not only these one-electron effects, but also of phonon-assisted tunneling[7,8]: the most elementary manifestation of a many-body tunneling phenomenon. Recent studies of tunneling into semiconductors have consisted of (the first) precision test of the one-electron model[9], use of this model to measure parameters characterizing the semiconductor energy band structure[10-13], further investigations of phonon-assisted tunneling[9,14-16], and the observation of the influence on the tunneling characteristics of electron-phonon interactions in the "bulk" part of a semiconductor electrode.[11,17] In this paper, we attempt to give an indication of the scope of recent efforts on semiconductor tunneling by surveying briefly the work on metal-semiconductor contacts published during 1968 and early 1969 (thereby supplementing an earlier, comprehensive review[18]).

The nature of the current flow across a metal-semiconductor contact is determined predominately by the one-electron potential-energy profile in the region of the contact. For contacts on group IV and III-V semiconductors, the value of the potential at the metal surface is caused primarily by the difference in the cohesive energies of the materials comprising the contact[18,19], and is approximately independent of the bias voltage applied across the contact[18,19]. The potential energy diagrams of a metal and a degenerate semiconductor are illustrated schematically in Fig. 1 for both the isolated electrons and the intimate contact. The extent of the space-charge region in the degenerate, n-type semiconductor is determined from the (prescribed) barrier height, V_b, at the interface and the density, n, of ionized donors in the space-charge region. For a uniform doping density one obtains[18,20] the Schottky-barrier model for a junction at x=0:

$$V(x) = [2\pi ne^2/\epsilon](x-d)^2 \tag{1a}$$

$$d = [\epsilon(V_b-eV)/2\pi ne^2]^{\frac{1}{2}} \tag{1b}$$

in which ϵ is the static dielectric constant of the semiconductor and V is the bias imposed across the junction. The image potential causes negligible effect on the tunneling in narrow junctions[11] and has been omitted from Eqs. (1).

In the limit of high and/or thick junctions [large V_b, small n] the current flows predominately via the mechanism of thermionic emission over the potential barrier as shown in Fig. 2 for the case that V>0. The contact rectifies in this limit with V>0 causing a lower barrier height hence large current flow. In the limit of low, thin barriers the tunneling mechanism of current flow predominates as indicated in the lower panel of Fig. 2. The junction also rectifies in this case but for small values of the bias ($eV \ll E_g$), the combined influence of the increasingly thinner barrier and inexhaustable reservoir of electrons in the metal causes V<0 to define the direction of large current flow. Rectification for this sign of the bias first was identified unambiguously by Padovani and Stratton[10] in 1966, forty-four years after its theoretical prediction[3-5] in 1932. The intermediate regime of low, thick junctions is characterized by "thermionic-field" emission[23,24]. The independent-electron description of specular tunneling in all three regimes has been reviewed recently by Padovani[25].

Despite the almost universal use in the literature of the one-electron, average-barrier model which we have just described, a critical, quantitative examination of the validity of this model has been performed only in the past year[9]. It is not self-evident that such a model ever describes experimental data. If the doping of semiconductor is large [$n > a_B^{-3}$, $a_B = \hbar^2 \varepsilon / m^* e^2$], then charge-density fluctuations in the space charge region can cause the failure of the junction potential to be described adequately by its average value. If the doping is low, [$n \lesssim a_B^{-3}$] then impurity-band (or hopping) conduction can cause the series resistance in the semiconductor electrode to dominates the electrical characteristics of the contact[26]. A survey[18] of experiments on semiconductor tunnel junctions indicates that the one-electron, average-barrier model almost always predicts a current density which is over an order-of magnitude below the experimental value. Therefore Steinrisser, Davis, and Duke[9] undertook a critical examination of the one-electron model description of tunneling into Ge:Sb, As. They used a phenomenological approach characterized by:

(1) The verification of the tunneling mechanism of current flow via the superconducting-electrode test[18] using superconducting metal contacts.

(2) The independent measurement of the parameters [m^*, ϵ, V_b and n] which characterize the (Schottky) barrier.

(3) Evaluation of the independent-electron specular tunneling characteristics by numerical methods which avoid any approximations once the model of the junction charge density has been selected.

Their junctions were fabricated by evaporating metal dots on vacuum-cleaved semiconductor surfaces. The conductance characteristic is defined to be the derivative of the current-voltage characteristic shown in the bottom panel of Fig. 2. It exhibits a minimum at $eV \cong \mu$ because for $eV > \mu$ the electron reservoir in the semiconductor is exhausted, i.e. no additional electrons become available for tunneling. A comparison[9] between the model calculation[27] for a Schottky barrier and experimental data is shown in Fig. 3. The absolute magnitude of the experimental conductance is uncertain by approximately $\pm$ 100% due to a 5% uncertainty in V_b. Therefore the agreement between the calculated and experimental characteristics is quite adequate for Ge:Sb in the doping range around $n \cong 8 \times 10^{18}$ cm^{-3}. The experimental results for Ge:As in this doping range compare less favorably with the model calculations.

Applications of tunneling measurements to determine the energy-momentum relation in the forbidden gap of the semiconductor have been performed in GaAs[10,11,13] and InAs[12]. The superconducting electrode test was not performed in any of these experiments. They were analyzed using approximate evaluations of the expression for the current through a

Schottky-barrier potential. Critiques of the analysis have been given by Conley and Mahan[11] and by Duke[18]. A comparison of the complete[27] Schottky-barrier analysis with data for metal contacts on Si:P, 4.5×10^{18} cm^{-3} $\leq n \leq 1.55 \times 10^{19}$ cm^{-3} has been given by Wolf and Losee[28] during the course of a study of zero-bias anomalies associated with localized, paramagnetic impurities at the edge of the space-charge barrier in the semiconductor. They also have performed a similar analysis[29] of contacts on CdS:In,Ga with doping in the range 1.7×10^{18} cm^{-3} $\leq n \leq 6 \times 10^{18}$. Although Wolf and Losee did not measure the barrier height V_b independently, they conclude that the shape of the experimental conductance data on the more heavily doped samples is described adequately by the complete Schottky-barrier analysis[27].

Many-body effects in electron tunneling usually are described using the transfer-Hamiltonian model[18]. The model Hamiltonian is given by

$$\mathcal{H} = \mathcal{H}_L + \mathcal{H}_R + \mathcal{H}_T \tag{2}$$

in which $\mathcal{H}_L$ and $\mathcal{H}_R$ describe the isolated left and right hand electrodes respectively, and $\mathcal{H}_T$ is a "transfer" term which describes the motion of an electron from one electrode to the other. In this model, a distinction is made between inelastic tunneling ["barrier-excitation"], described by (e.g.) electron-phonon interaction terms in $\mathcal{H}_T$, and electrode "self-energy" effects, associated with (e.g.) electron-phonon interaction terms in $\mathcal{H}_L$ or $\mathcal{H}_R$. Some phenomena, like tunneling into a superconducting metal contact, clearly fall into one of these two categories [self-energy effects in that case]. If, however, structure in the tunneling characteristic is observed for values of the bias near an optical phonon energy in the semiconductor, it is not obvious *a priori* that the distinction between "barrier" and "electrode" effects is a useful concept for the interpretation of such observations. Its utility is based on the extent to which the two types of mechanisms predict distinguishable features in the tunneling characteristics. If we consider deformation-potential interactions of the electron with optical phonons, then the electron-phonon interaction vertex is given by:

$$V_{\underset{\sim}{q}} = \text{const} \tag{3}$$

and the two mechanisms predict different characteristics structures in the conductance [$G = dI/dV$] and in d^2I/dV^2 as shown in Fig. 4. In this case, for which the electron-phonon interaction is independent of the momentum transfer, $\underset{\sim}{q}$, to the phonon, the electrode interactions cause an approximately *symmetric* structure in d^2I/dV^2 about zero bias whereas the barrier interactions [i.e. inelastic tunneling] always cause an antisymmetric structure in d^2I/dV^2 about zero bias. This distinction based on symmetry is peculiar to the form (3) for the interaction vertex. In general, all that can be said[18,30] is that inelastic tunneling always causes approximately symmetrical threshold increases in dI/dV whereas electrode interactions cause cusp-like behavior in dI/dV at $eV = \pm\hbar\omega_o$ for (dispersionless) bosons of energy $\hbar\omega_o$.

The essential feature of interactions in the barrier is their stimulation of an additional current flow proportional to the number of opportunities for an electron to both tunnel and simultaneously create an elementary excitation in the barrier. The kinematics of these inelastic tunneling processes are outlined in Fig. 5. The sharp step in the conductance at $eV = \pm \hbar\omega_o$ for optical phonons is seen to be a consequence of the sharp peak in the optical phonon density of states at $\epsilon \cong \hbar\omega_o$ for optical phonons is seen to be a consequence of the sharp peak in the optical phonon density of states at $\epsilon \cong \hbar\omega_o$. The emission of acoustical phonons leads to a minimum in the conductance near zero bias, which seems to have been observed in several systems[14-16]. However, the topic of acoustical phonon emission in direct-band gap semiconductors is currently a controversial one[18].

The one case in which phonon-assisted tunneling has been observed unambiguously in metal-semiconductor contacts is that of tunneling into the indirect semiconductors germanium[9] and silicon[31]. In these semiconductors, the inelastic phonon emission occurs with a large change in the quasimomentum of the electron, just as in the case of p-n tunnel diodes[7,8,18]. An example of the experimental tunnel characteristics is shown in Fig. 6. The experimental lineshapes are in semiquantitative agreement[9] with a model calculation in which the tunneling process may be regarded as consisting of two stages. An electron in the metal contact first tunnels into an evanescent state composed of a superposition of Bloch waves with quasimomenta near Γ (i.e. $\underset{\sim}{k} \cong 0$). Then it emits a phonon and is transferred to one of the conduction band minima near the L points $[\underset{\sim}{k} = (\pi/a)(111)]$ in the Brillouin zone. In p-n tunnel diodes other mechanisms for the phonon emission have been considered[18] with the one analogous to that described above being proposed in that case by Kleinman[32]. The optical-phonon contributions to the characteristics shown in Fig. 6 are in accordance with our expectations from Fig. 5. The sharp steps in the conductance [as opposed to a gradually rising conductance $G_{ph}(V) \propto V^2$] associated with acoustical phonons are due to the fact that the electrons can be transferred from Γ to L in the semiconductor only by emitting a phonon of quasimomentum $\underset{\sim}{k} \cong -\underset{\sim}{k}_L$. As these phonons have an energy, $\epsilon_\lambda = \hbar\omega_\lambda(-\underset{\sim}{k}_L)$, we find that momentum conservation restricts the vertex function, $V_\lambda(\epsilon)$, [for electron-phonon coupling to the λ branch of the phonon spectrum] to be zero for $\epsilon < \epsilon_\lambda$. Therefore, provided the appropriate conservation laws are incorporated into the vertex function, the considerations shown in Fig. 5 apply to this case also.

The essential ingredient of phonon self-energy effects in the semiconductor electrode is the modification of the "bulk" electronic spectral density by the electron-phonon interaction[17,18]. As the specular tunnel conductance is proportional[18] to the number of electronic states associated with a specified electron energy, $E = \epsilon + \zeta$, phonon-induced changes in the number of these states affect the tunneling characteristics. The nature of this effect is indicated schematically in Fig. 7. The conductance, G(V), is associated with electrons of energy E = eV in the semiconductor. In the case of an electron-phonon vertex of the form given by Eq. (3), only the change in the energy-momentum relation of the electron (due to the electron-phonon interaction) enters the evaluation of the conductance. For the model illustrated in

Fig. (7),

$$G(V) = \text{const.}\ x[\hbar^2 k^2(\epsilon=-eV)/2m^*] \qquad (4)$$

in which the dependence of $G(V)$ on $k^2(-eV)$ is due to the phase-space weighting of initial (or final) states for tunneling.[18,30] When $\epsilon \to -\hbar\omega_o$, the phonon-modified electronic dispersion relation, $\epsilon(\underset{\sim}{k})$, gives an unusually small value of $k^2(\epsilon)$ as shown in Fig. 7b. Therefore $G(V)$ exhibits a dip at $eV = \hbar\omega_o$ associated with $\epsilon \to -eV$ in Eq. (4). The inverse effect occurs at $\epsilon \to +eV$ giving the antisymmetric tunnel characteristics shown in Fig. 4 and in Fig. 7c. A comparison of the predicted value of d^2I/dV^2 [compare, e.g. with Fig. 4] and the measured value in In/oxide/Si:B junctions is shown in Fig. 8. Corrections to the experimental data considerably improve the agreement at $eV \cong -\hbar\omega_o$ between the data and the calculation[17b]. Observations of this phenomenon were reported first[11] for contacts on n-type GaAs. Fig. 8 shows data taken on the metal-oxide-silicon system whose study was initiated by Wolf[33]. The observation of similar self-energy effects also has been reported in p-type GaAs[34].

Several generalizations of Eqs. (3) and (4) are used in the literature. The bias and energy dependence of the (independent-electron) barrier penetration probability was incorporated into the analysis of Davis and Duke by means of the plausible ansatz[17b] that this probability depends only on the electronic energy variable, ϵ, and parallel component of momentum, $\underset{\sim}{k}_{11}$. This prescription subsequently has been justified by Davis[35] and independently by Appelbaum and Brinkman[36]. The effect on the tunnel characteristics of the $\underset{\sim}{q}$ dependence of the electron-boson vertex also has been examined in more detail for polar electron-phonon coupling[17b] and electron-plasmon interactions[30,37]. These analysis have been applied to describe data taken using metal contacts on n-type CdS[17b,29] and GaAs[37] respectively. Inelastic plasmon excitation in GaAs also has been identified tentatively[30,38].

Summarizing, we have surveyed briefly the recent (1968-69) literature on tunneling spectroscopy in metal-semiconductor contacts. Highlights of this work include a precision test of the one-electron model[9], various types of phonon spectroscopy[9,11,14-16,39], examinations of the consequences, both experimental[11,29,33,34,37] and theoretical[11,17,18,30,35-37] of electronic self-energy effects in the semiconductor electrode, studies of zero-bias anomalies associated with paramagnetic impurities[28], and various applications[11-13,28,29,40-42] (as opposed to critical tests) of the Schottky-barrier model of one-electron tunneling. Future directions of this field include more extensive and higher-precision spectroscopic studies of electrons and elementary excitations (phonons, plasmons, magnons) in semiconductors, and examinations of more specifically "surface" effects associated with potential-fluctuations, magnetic impurities, and trapping states[43] in the junction region.

1. L. Esaki, Phys. Rev. 109, 603 (1957).

2. J. Frenkel, Phys. Rev. 36, 1604 (1930).

3. A.H. Wilson, Proc. Roy. Soc. (London) A136, 487 (1932).

4. J. Frenkel and A. Joffe, Phys. Z. Sowjetunion, 1, 60 (1932).

5. L. Nordheim, Z. Phys. 75, 434 (1932).

6. C. Zener, Proc. Roy. Soc. (London) A145, 523 (1934).

7. N. Holonyak, I.A. Lesk, R.N. Hall, J.J. Tiemann, and H. Ehrenreich, Phys. Rev. Letters 3, 167 (1959).

8. L. Esaki and Y. Miyahara, Solid State Electron. 2, 13 (1960).

9. F. Steinrisser, L.C. Davis, and C.B. Duke, Phys. Rev. 176, 912 (1968).

10. F.A. Padovani and R. Stratton, Phys. Rev. Letters 16, 1202 (1966).

11. J.W. Conley and G.D. Mahan, Phys. Rev. 161, 681 (1967).

12. G.H. Parker and C.A. Mead, Phys. Rev. Letters 21, 605 (1968).

13. M.F. Millea, M. McColl, and C.A. Mead, Phys. Rev. 177, 1164 (1969).

14. C.B. Duke, S.D. Silverstein, and A.J. Bennett, Phys. Rev. Letters 19, 312 (1967).

15. P. Thomas and H.J. Quiesser, Phys. Rev. 176, 983 (1968).

16. A.J. bennett, C.B. Duke, and S.D. Silverstein, Phys. Rev. 176, 969 (1968).

17a. L.C. Davis and C.B. Duke, Solid State Comm. 6, 193 (1968)

17b. L.C. Davis and C.B. Duke, Phys. Rev. (to be published).

18. C.B. Duke, *Tunneling in Solids* (Academic Press, New York, 1969).

19. C.B. Duke, J. Vac. Sci. Tech. 6, 152 (1969).

20. H.K. Henisch, Rectifying Semiconductor Contacts (Clarendon Press, Oxford, 1957), chpt. 7.

21. N.F. Mott, Proc. Roy. Soc. (London) A171, 27 (1939); A171, 281 (1939).

22. W. Schottky, Z. Physik 113, 307 (1939); 118, 539 (1939).

23. R. Stratton, Phys. Rev. 125, 67 (1962).

24. F. Padovani and R. Stratton, Solid State Electron 9, 695 (1966).

25. F. Padovani in Semiconductors and Semimetals, Vol. 6 (Academic Press, in preparation).

26. M.N. Alexander and D.F. Holcomb, Rev. Mod. Phys. 40, 815 (1968).

27. J.W. Conley, C.B. Duke, G.D. Mahan, and J.J. Tiemann, Phys. Rev. 150, 466 (1966).

28. E.L. Wolf and D.L. Losee, Solid State Comm. (to be published).

29. D.L. Losee and E.L. Wolf, Phys. Rev. (to be published).

30. C.B. Duke, Phys. Rev. Comments and Addenda (to be published).

31. E.L. Wolf, unpublished.

32. L. Kleinman, Phys. Rev. 140, A637 (1965).

33. E.L. Wolf, Phys. Rev. Letters 20, 204 (1968).

34. D.C. Tsui, Phys. Rev. Letters 21, 994 (1968).

35. L.C. Davis, Solid State Comm. (to be published).

36. J.A. Appelbaum and W. Brinkman, Phys. Rev. (to be published).

37. C.B. Duke, M.J. Rice, and F. Steinrisser, Phys. Rev. (to be published)

38. D.C. Tsui, Phys. Rev. Letters 22, 293 (1969).

39. W.A. Thompson, Phys. Rev. Letters 20, 1085 (1968).

40. H.F. Tao and Y. Hsia, Appl. Phys. Lett. 13, 291 (1968).

41. A.N. Saxena, Appl. Phys. Lett. 14, 11 (1969).

42. C.R. Crowell and V.L. Rideout, Appl. Phys. Lett. 14, 85 (1969).

43. G.H. Parker and C.A. Mead, Appl. Phys. Lett. 14, 21 (1969); (to be published).

FIGURE CAPTIONS

Figure 1: (a) Schematic potential-energy versus distance diagram both for an isolated metal electrode of Fermi energy E_F and work function ϕ and for an isolated degenerate semiconductor electrode with electron affinity $\chi+\mu$ and (impurity-induced) Fermi degeneracy μ.

(b) Schematic potential-energy versus distance diagram of an intimate contact of the electrodes shown in Fig. 1. The order of magnitude of the parameters for a "typical" tunnel junction is indicated in the figure.

Figure 2: Schematic illustration of current flow in a metal-semiconductor contact and of the mechanisms of current flow for high, thick junctions (thermionic emission) as opposed to low, thin junctions (tunnel or internal-field emission).

Figure 3: Comparison between three experimentally measured conductance curves on $n = 7.5\times10^{18}/cm^3$ Sb-doped Ge [solid lines (a), (c), and (d)] at 4.2°K and the calculated conductance [dashed line (b)] using the model developed by Conley et. al. (ref. 27) for a barrier height $V_b = 0.63$ eV obtained from capacitance measurements. The most commonly observed conductance curves were similar to (c), whereas (a) and (d) represent the high- and the low- conductance extremes. The contact metal is Pb and the contact area is $2.5\pm0.5\times10^{-4}$ cm^2. Structure associated with the superconducting energy gap has been omitted. The Fermi degeneracy $\mu = 25$ meV has been indicated. After Steinrisser, Davis, and Duke, ref. 9.

Figure 4: Schematic illustration of the distinction between the tunneling characteristics associated with interactions in the barrier [described by $\mathcal{H}_T$ and labeled inelastic tunneling] and those associated with interactions in the electrodes [described by $\mathcal{H}_L$ and/or $\mathcal{H}_R$]. The illustrated curves are drawn for a model of a metal-semiconductor contact in which interactions in the metal are neglected and the electrons in the semiconductor interact with dispersionless optical phonons via a vertex of the form given by Eq. (3) in the text.

Figure 5: Schematic description of the nature of a barrier-excitation (i.e. "inelastic tunneling") process, and outline of the kinematical evaluation of the conductance G. $N_b(\epsilon)$ is the density of states for the barrier excitations, and $V(\epsilon)$ is the electron-excitation vertex for an excitation of energy ϵ.

Figure 6: Conductance and d^2I/dV^2 of an indium contact on As-doped Ge junctions at 2^oK. The arsenic doping is $n = 7.0\times10^{18}/cm^3$. The observation of the indium superconducting gap at zero bias is shown explicitly. Its presence shifts the phonon structure to higher energies by approximately $\Delta = 0.5$ meV. (After Steinrisser, Davis, and Duke, ref. 9.)

Figure 7: (a) Schematic potential energy versus distance diagram for a metal-insulator-semiconductor junction. Energies are measured from the bottom of the semiconductor band, and ζ denotes the Fermi degeneracy of the semiconductor.

(b) Dispersion relation for electrons in the (degenerate) semiconductor electrode interacting with optical phonons of energy $\hbar\omega_o$. The heavy dashed line indicates the dispersion relation in the absence of electron-phonon interactions.

(c) The conductance of the metal-insulator-semiconductor tunnel junction shown in Fig. 7a evaluated using a constant-barrier-penetration factor model. The dashed line shows the conductance predicted by this model in the absence of electron-phonon interactions in the (bulk) semiconductor electrode. (After Davis and Duke, ref. 17b.)

Figure 8: Comparison of theoretical (dashed line) and experimental (solid line) d^2I/dV^2 characteristic for an indium/oxide/silicon:Boron junction. The resonant structure at $eV = \pm\hbar\omega_o$ is attributed to electron-phonon interactions in the semiconductor electrodes. The parameters refer to Eqs. (1.8), (2.3), (2.5) and (A.2.6) in ref. 17b. (After Davis and Duke, ref. 17b.)

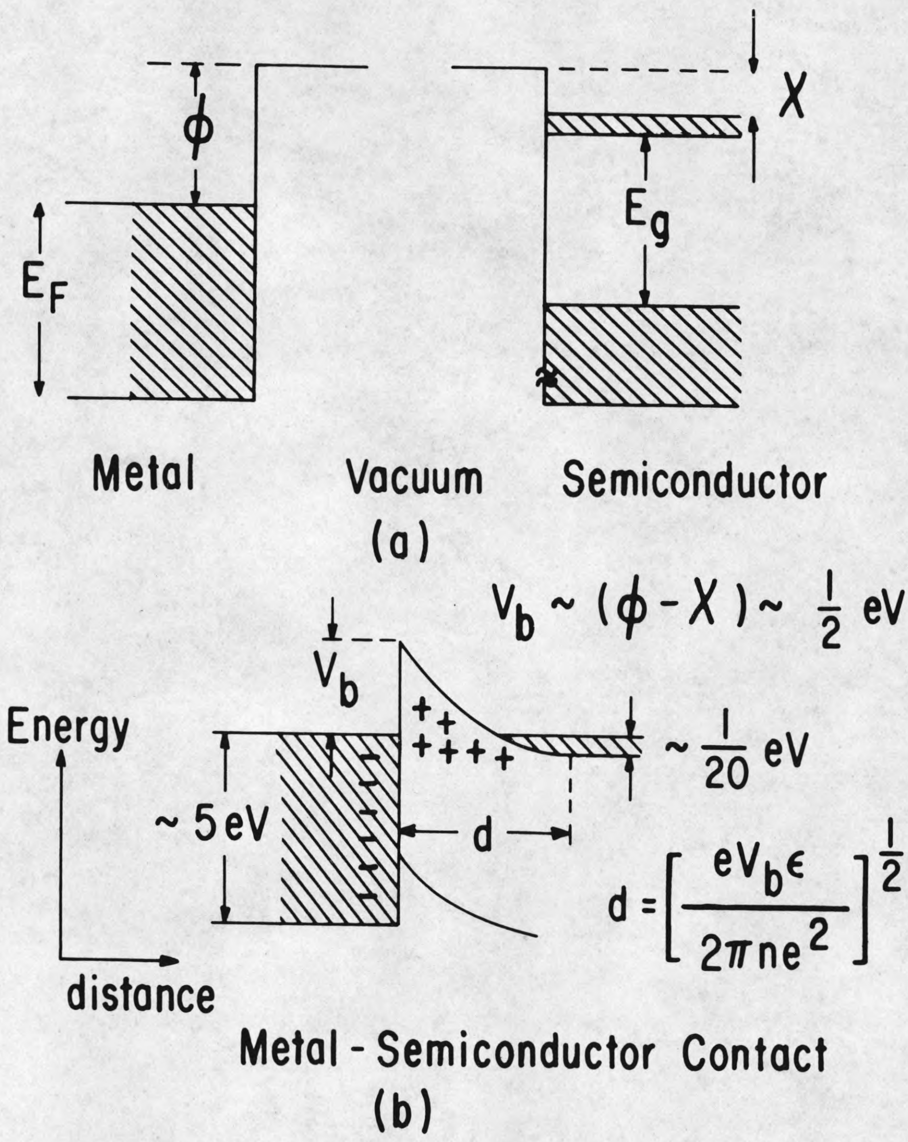
φ
χ
E_g
E_F
Metal
Vacuum
Semiconductor
(a)
$V_b \sim (\phi - \chi) \sim \frac{1}{2}$ eV
V_b
Energy
$\sim \frac{1}{20}$ eV
~ 5 eV
d
$d = \left[\frac{eV_b \epsilon}{2\pi n e^2}\right]^{\frac{1}{2}}$
distance
Metal - Semiconductor Contact
(b)

Figure 1

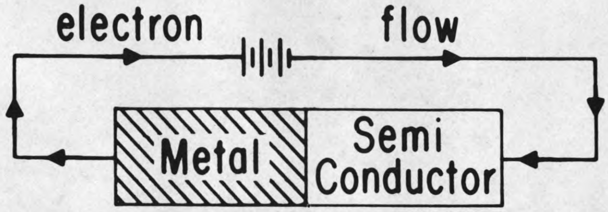

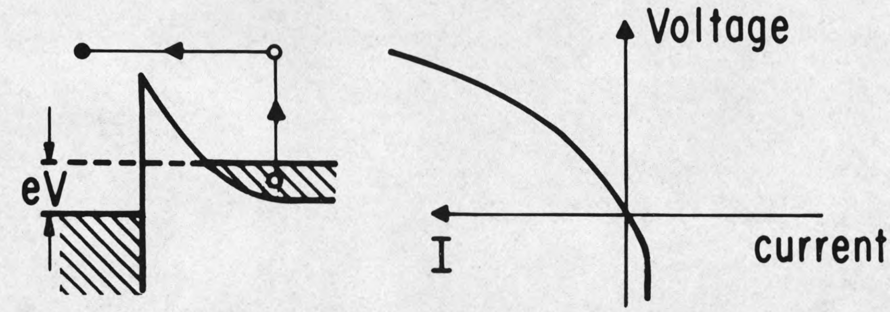

Thermionic Current Flow (Mott, Schottky, 1939)

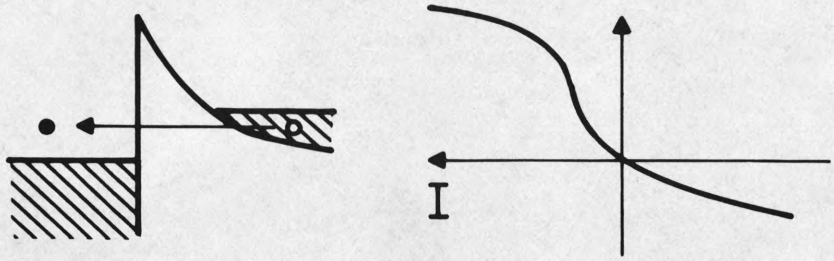

Tunneling Current Flow (Wilson, Frenkel and Joffe, Nordheim, 1932)

Figure 2

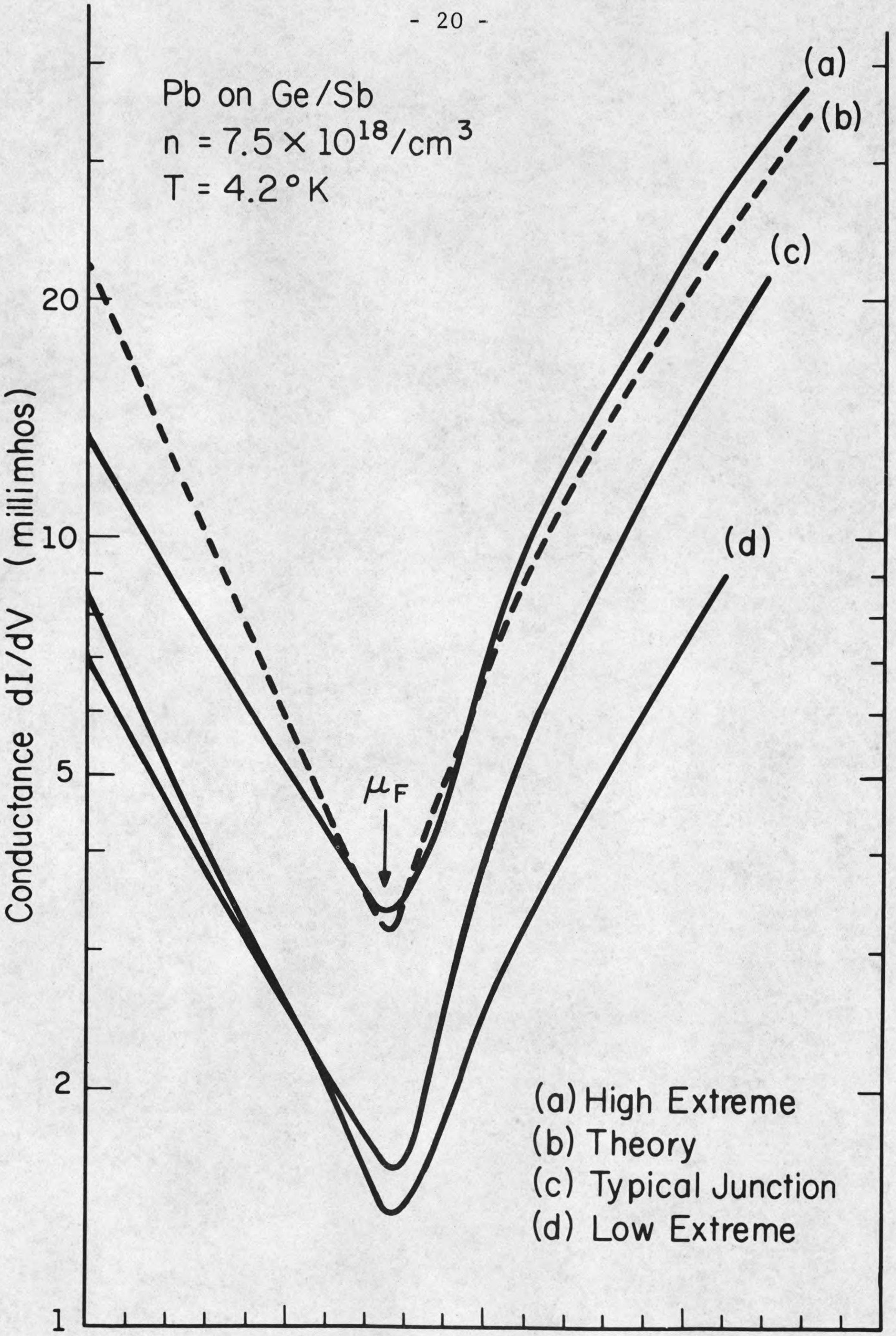

Pb on Ge/Sb
n = 7.5 × 10^18/cm^3
T = 4.2°K
(a)
(b)
(c)
(d)
μF
20
10
5
2
1
-100
-50
0
50
100
Conductance dI/dV (millimhos)
Bias Voltage (mV)
(a) High Extreme
(b) Theory
(c) Typical Junction
(d) Low Extreme

Figure 3

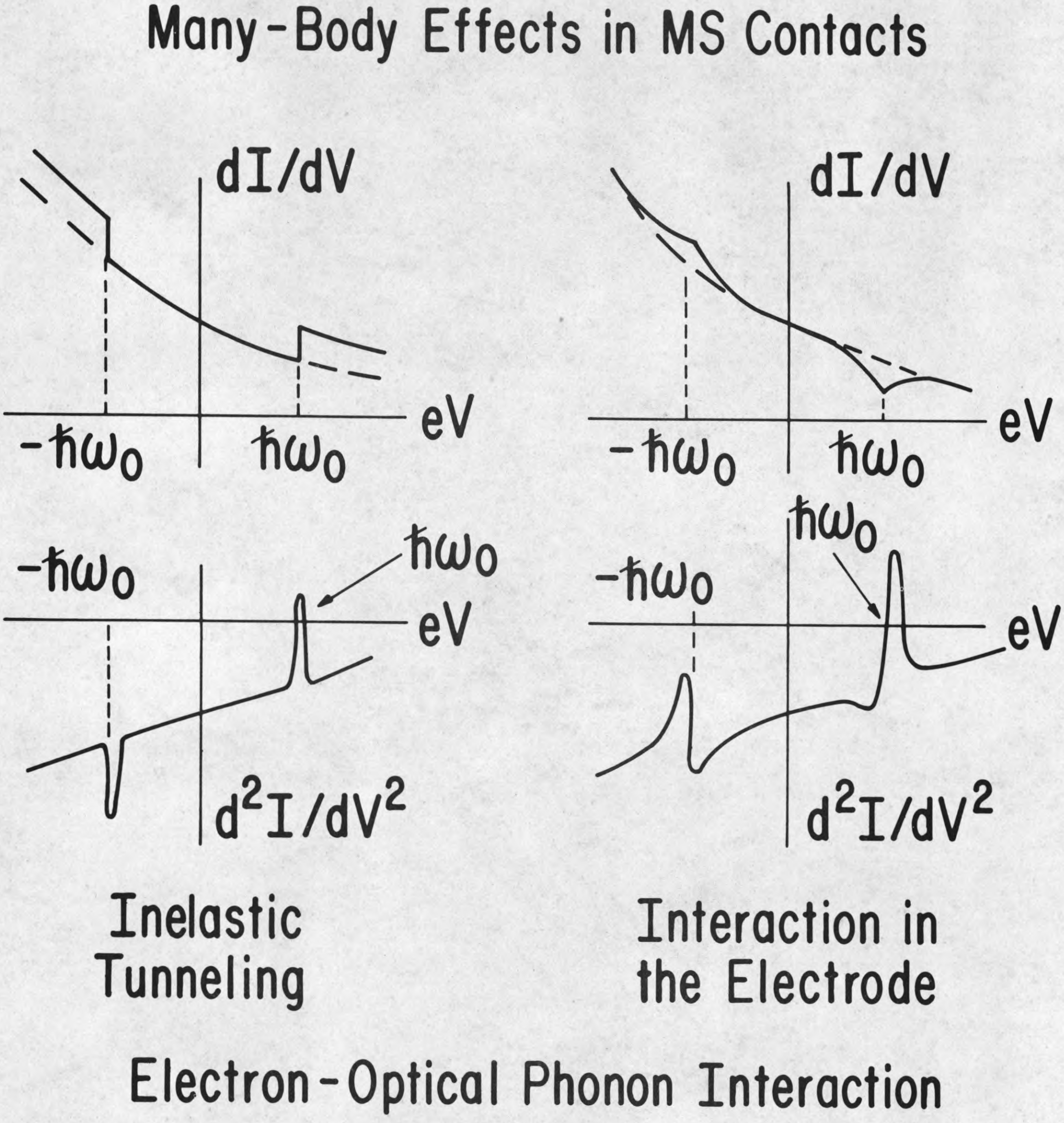
Many-Body Effects in MS Contacts
dI/dV
eV
$-\hbar\omega_0$
$\hbar\omega_0$
dI/dV
eV
$-\hbar\omega_0$
$\hbar\omega_0$
$-\hbar\omega_0$
$\hbar\omega_0$
eV
d^2I/dV^2
$\hbar\omega_0$
$-\hbar\omega_0$
eV
d^2I/dV^2
Inelastic Tunneling
Interaction in the Electrode
Electron-Optical Phonon Interaction

Figure 4

KINEMATICS OF BARRIER-EXCITATION SPECTROSCOPY

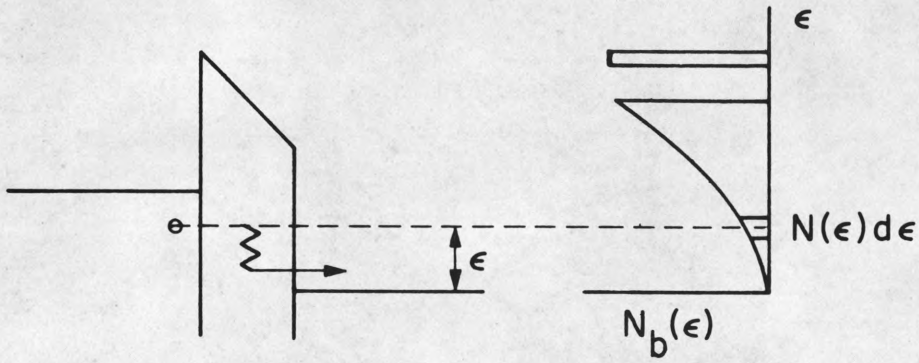

G = CHANGE IN CURRENT DUE TO CHANGE IN BIAS

$\propto$ NUMBER OF NEW POSSIBLE "CHANNELS" FOR TUNNELING

$$\propto \int_0^{|eV|} N_b(\epsilon)\, d\epsilon \cdot |V(\epsilon)|^2$$

$$\frac{dG}{dV} = \frac{d^2J}{dV^2} \propto N_b(eV)$$

Figure 5

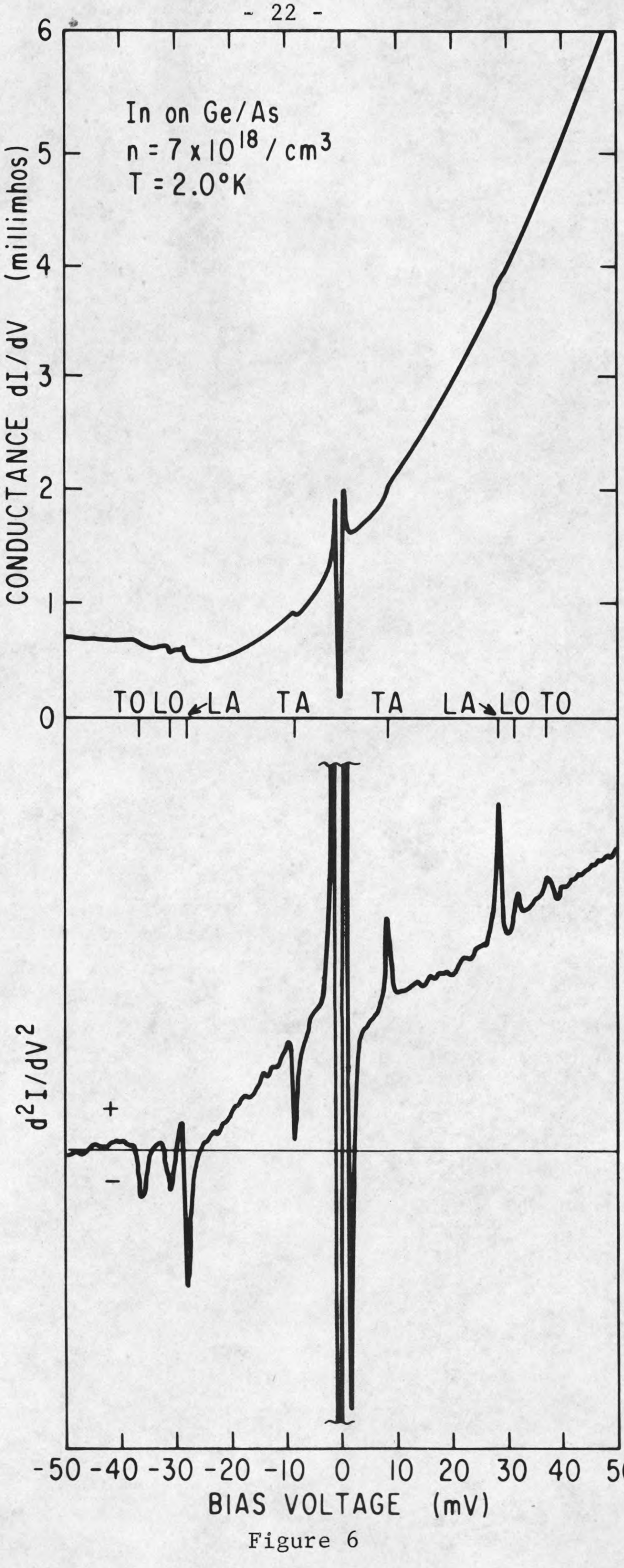
In on Ge/As
n = 7 x 10^18 / cm^3
T = 2.0°K
CONDUCTANCE dI/dV (millimhos)
0
1
2
3
4
5
6
TO LO LA TA TA LA LO TO
d^2I/dV^2
+
-
-50 -40 -30 -20 -10 0 10 20 30 40 50
BIAS VOLTAGE (mV)

Figure 6

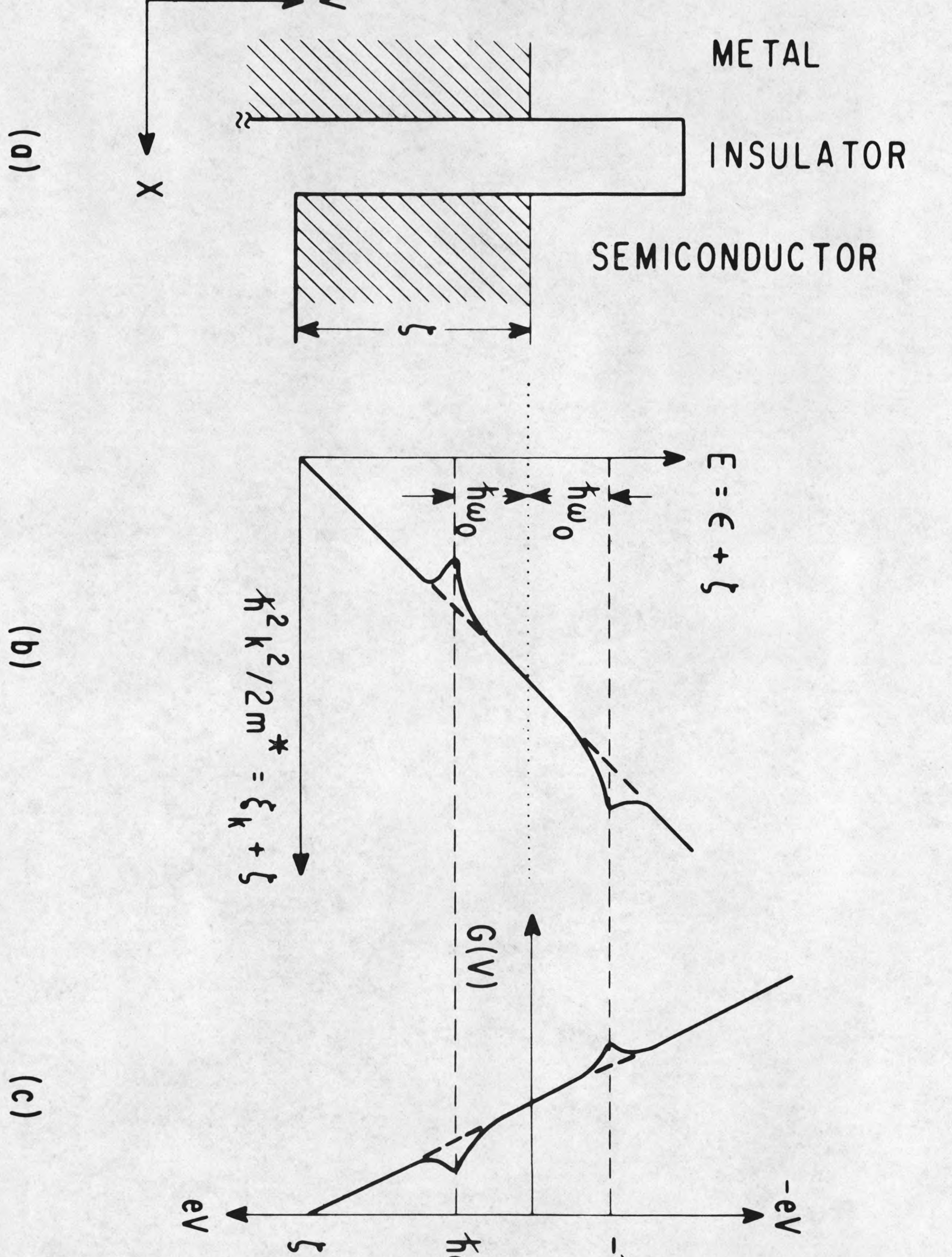
(a)
V
X
METAL
INSULATOR
SEMICONDUCTOR
ζ
(b)
$E = \epsilon + \zeta$
$\hbar\omega_0$
$\hbar\omega_0$
$\hbar^2 k^2/2m^* = \xi_k + \zeta$
(c)
G(V)
eV
-eV
ζ
$\hbar\omega_0$
$-\hbar\omega_0$

Figure 7

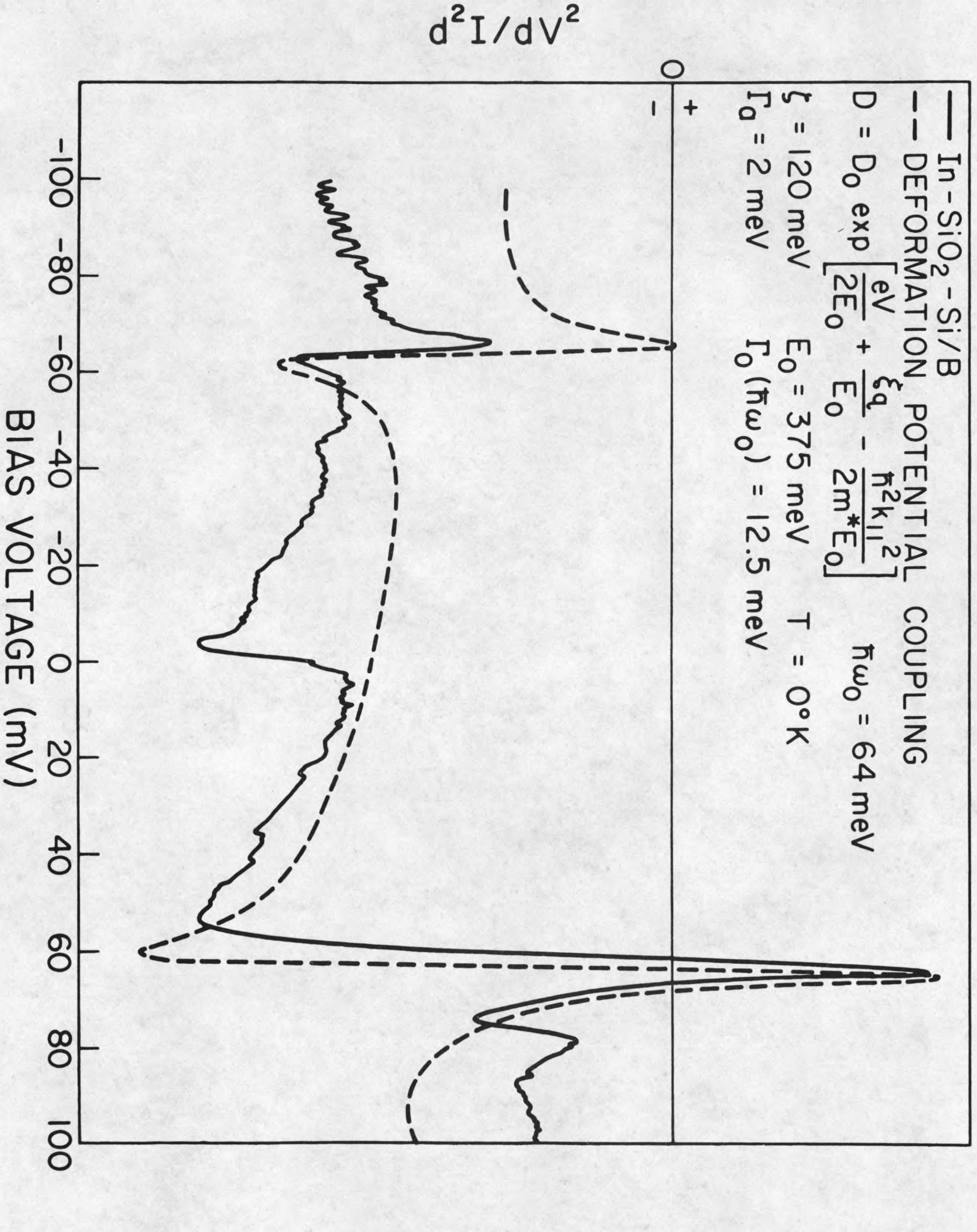

d^2I/dV^2
0
+
−
— In-SiO_2-Si/B
-- DEFORMATION POTENTIAL COUPLING
$D = D_0 \exp\left[\frac{eV}{2E_0} + \frac{\xi q}{E_0} - \frac{\hbar^2 k_{\parallel}^2}{2m^* E_0}\right]$ $\hbar\omega_0 = 64$ meV
$\xi = 120$ meV $E_0 = 375$ meV T = 0°K
$\Gamma_a = 2$ meV $\Gamma_0(\hbar\omega_0) = 12.5$ meV
-100 -80 -60 -40 -20 0 20 40 60 80 100
BIAS VOLTAGE (mV)

Figure 8

Distribution List as of August 1, 1969

Dr A.A. Dougal
Asst Director (Research)
Ofc of Defense Res & Eng
Department of Defense
Washington, D.C. 20301

Office of Deputy Director
(Research and Information, Rm 3D1037)
Department of Defense
The Pentagon
Washington, D.C. 20301

Director, Advanced Research Projects
Agency
Department of Defense
Washington, D.C. 20301

Director for Materials Sciences
Advanced Research Projects Agency
Department of Defense
Washington, D.C. 20301

Headquarters
Defense Communications Agency (340)
Washington, D.C. 20305

Defense Documentation Center
Attn: DDC-TCA
Cameron Station
Alexandria, Virginia 22314 (50 Copies)

Director
National Security Agency
Attn: TDL
Fort George G. Meade, Maryland 20755

Weapons Systems Evaluation Group
Attn: Colonel Blaine O. Vogt
400 Army-Navy Drive
Arlington, Virginia 22202

Central Intelligence Agency
Attn: OCR/DD Publications
Washington, D.C. 20505

Hq USAF (AFRDD)
The Pentagon
Washington, D.C. 20330

Hq USAF (AFRDDG)
The Pentagon
Washington, D.C. 20330

Hq USAF (AFRDSD)
The Pentagon
Washington, D.C. 20330

Colonel E.P. Gaines, Jr.
ACDA/FO
1901 Pennsylvania Ave N.W.
Washington, D.C. 20451

Lt Col R.B. Kalisch (SREE)
Chief, Electronics Division
Directorate of Engineering Sciences
Air Force Office of Scientific Research
Arlington, Virginia 22209

Dr I.R. Mirman
AFSC (SCT)
Andrews Air Force Base, Maryland 20331

AFSC (SCTSE)
Andrews Air Force Base, Maryland 20331

Mr Morton M. Pavane, Chief
AFSC Scientific and Technical Liaison Office
26 Federal Plaza, Suite 1313
New York, New York 10007

Rome Air Development Center
Attn: Documents Library (EMTLD)
Griffiss Air Force Base, New York 13440

Mr H.E. Webb (EMMIIS)
Rome Air Development Center
Griffiss Air Force Base, New York 13440

Dr L.M. Hollingsworth
AFCRL (CRN)
L.G. Hanscom Field
Bedford, Massachusetts 01730

AFCRL (CRMPLR), Stop 29
AFCRL Research Library
L.G. Hanscom Field
Bedford, Massachusetts 01730

Hq ESD (ESTI)
L.G. Hanscom Field
Bedford, Massachusetts 01730 (2 copies)

Professor J. J. D'Azzo
Dept of Electrical Engineering
Air Force Institute of Technology
Wright-Patterson AFB, Ohio 45433

Dr H.V. Noble (CAVT)
Air Force Avionics Laboratory
Wright-Patterson AFB, Ohio 45433

Director
Air Force Avionics Laboratory
Wright-Patterson AFB, Ohio 45433

AFAL (AVTA/R.D. Larson
Wright-Patterson AFB, Ohio 45433

Director of Faculty Research
Department of the Air Force
U.S. Air Force Academy
Colorado Springs, Colorado 80840

Academy Library (DFSLB)
USAF Academy
Colorado Springs, Colorado 80840

Director
Aerospace Mechanics Division
Frank J. Seiler Research Laboratory (OAR)
USAF Academy
Colorado Springs Colorado 80840

Director, USAF PROJECT RAND
Via: Air Force Liaison Office
The RAND Corporation
Attn: Library D
1700 Main Street
Santa Monica, California 90045

Hq SAMSO (SMTTA/Lt Nelson)
AF Unit Post Office
Los Angeles, California 90045

Det 6, Hq OAR
Air Force Unit Post Office
Los Angeles, California 90045

AUL3T-9663
Maxwell AFB, Alabama 36112

AFETR Technical Library
(ETV, MU-135)
Patrick AFB, Florida 32925

ADTC (ADBPS-12)
Eglin AFB, Florida 32542

Mr B.R. Locke
Technical Adviser, Requirements
USAF Security Service
Kelly Air Force Base, Texas 78241

Hq AMD (AMR)
Brooks AFB, Texas 78235

USAFSAM (SMKOR)
Brooks AFB, Texas 78235

Commanding General
Attn: STEWS-RE-L, Technical Library
White Sands Missile Range
New Mexico 88002 (2 copies)

Hq AEDC (AETS)
Attn: Library/Documents
Arnold AFS, Tennessee 37389

European Office of Aerospace Research
APO New York 09667

Phsical & Engineering Sciences Division
U.S. Army Research Office
3045 Columbia Pike
Arlington, Virginia 22204

Commanding General
U.S. Army Security Agency
Attn: IARD-T
Arlington Hall Station
Arlington, Virginia 22212

Commanding General
U.S. Army Materiel Command
Attn: AMCRD-TP
Washington, D.C. 20315

Technical Director (SMUFA-A2000-107-1)
Frankford Arsenal
Philadelphia, Pennsylvania 19137

Redstone Scientific Information Center
Attn: Chief, Document Section
U.S. Army Missile Command
Redstone Arsenal, Alabama 35809

Commanding General
U.S. Army Missile Command
Attn: AMSMI-REX
Redstone Arsenal, Alabama 35809

Commanding General
U.S. Army Strategic Communications Command
Attn: SCC-CG-SAE
Fort Huachuca, Arizona 85613

Commanding Officer
Army Materials and Mechanics Res. Center
Attn: Dr H. Priest
Watertown Arsenal
Watertown, Massachusetts 02172

Commandant
U.S. Army Air Defense School
Attn: Missile Science Division, C&S Dept
P.O. Box 9390
Fort Bliss, Texas 79916

Commandant
U.S. Army Command & General Staff College
Attn: Acquisitions, Library Division
Fort Leavenworth, Kansas 66027

Commanding Officer
U.S. Army Electronics R&D Activity
White Sands Missile Range, New Mexico 88002

Mr Norman J. Field, AMSEL-RD-S
Chief, Office of Science & Technology
Research and Development Directorate
U.S. Army Electronics Command
Fort Monmouth, New Jersey 07703

Commanding Officer
Harry Diamond Laboratories
Attn: Dr Berthold Altman (AMXDO-TI)
Connecticut Avenue and Van Ness St N.W.
Washington, D.C. 20438

Director
Walter Reed Army Institute of Research
Walter Reed Army Medical Center
Washington, D.C. 20012

Commanding Officer (AMXRD-BAT)
U.S. Army Ballistics Research Laboratory
Aberdeen Proving Ground
Aberdeen, Maryland 21005

Technical Director
U.S. Army Limited War Laboratory
Aberdeen Proving Ground
Aberdeen, Maryland 21005

Commanding Officer
Human Engineering Laboratories
Aberdeen Proving Ground
Aberdeen, Maryland 21005

U.S. Army Munitions Command
Attn: Science & Technology Br. Bldg 59
Picatinny Arsenal, SMUPA-VA6
Dover, New Jersey 07801

U.S. Army Mobility Equipment Research
and Development Center
Attn: Technical Document Center, Bldg 315
Fort Belvoir, Virginia 22060

Director
U.S. Army Engineer Geodesy,
Intelligence & Mapping
Research and Development Agency
Fort Belvoir, Virginia 22060

Dr Herman Robl
Deputy Chief Scientist
U.S. Army Research Office (Durham)
Box CM, Duke Station
Durham, North Carolina 27706

Richard O. Ulsh (CRDARD-IPO)
U.S. Army Research Office (Durham)
Box CM, Duke Station
Durham, North Carolina 27706

Mr Robert O. Parker, AMSEL-RD-S
Executive Secretary, JSTAC
U.S. Army Electronics Command
Fort Monmouth, New Jersey 07703

Commanding General
U.S. Army Electronics Command
Fort Monmouth, New Jersey 07703
Attention:AMSEL-SC
RD-GF
RD-MT
XL-D
XL-E
XL-C
XL-S (Dr R. Buser)
HL-CT-DD
HL-CT-R
HL-CT-L (Dr W.S. McAfee)
HL-CT-O
HL-CT-I
HL-CT-A
NL-D
NL-A
NL-P
NL-P-2 (Mr D. Haratz)
NL-R (Mr R. Kulinyi)
NL-S
KL-D
KL-E
KL-S (Dr H. Jacobs)
KL-SM (Drs Schiel/Hieslmair)
KL-T
VL-D
VL-F (Mr R.J. Niemela)
WL-D

1 copy to each symbol listed individually addressed

Dr A.D. Schnitzler, AMSEL-HL-NVII
Night Vision Laboratory, USAECOM
Fort Belvoir, Virginia 22060

Dr G.M. Janney, AMSEL-HL-NVOR
Night Vison Laboratory,USAECOM
Fort Belvoir, Virginia 22060

Atmospheric Sciences Office
Atmospheric Sciences Laboratory
White Sands Missile Range
New Mexico 88002

Missile Electronic Warfare,
Technical Area, AMSEL-WT-MT
White Sands Missile Range
New Mexico 88002

Project Manager
Common Positioning & Navigation Systems
Attn: Harold H. Bahr (AMCPM-NS-TM), Bldg 439
U.S. Army Electronics Command
Fort Monmouth, New Jersey 07703

Director, Electronic Programs
Attn: Code 427
Department of the Navy
Washington, D.C. 20360

Commander
U.S. Naval Security Group Command
Attn: G43
3801 Nebraska Avenue
Washington, D.C. 20390

Director
Naval Research Laboratory
Washington, D.C. 20390
Attn: Code 2027 6 copies
Dr W.C. Hall, Code 7000 1 copy
Dr A. Brodizinsky, Sup.Elec Div. 1 copy

Dr G.M.R. Winkler
Director, Time Service Division
U.S. Naval Observatory
Washington, D.C. 20390

Naval Air Systems Command
AIR 03
Washington, D.C. 20360 2 copies

Naval Ship Systems Command
Ship 031
Washington, D.C. 20360

Naval ship Systems Command
Ship 035
Washington, D.C. 20360

U.S. Naval Weapons Laboratory
Dahlgren, Virginia 22448

Naval Electronic Systems Command
ELEX 03, Room 2046 Munitions Building
Department of the Navy
Washington, D.C. 20360 (2 copies)

Commander
Naval Electronics Laboratory Center
Attn: Library
San Diego, California 92152 (2 copies)

Deputy Director and Chief Scientist
Office of Naval Research Branch Office
1030 Est Gree Street
Pasadena, California 91101

Library (Code2124)
Technical Report Section
Naval Postgraduate School
Monterey, California 93940

Glen A. Myers (Code 52Mv)
Assoc Professor of Elec. Engineering
Naval Postgraduate School
Monterey, California 93940

Commanding Officer and Director
U.S. Naval Underwater Sound Laboratory
Fort Trumbull
New London, Connecticut 06840

Commanding Officer
Naval Avionics Facility
Indianapolis, Indiana 46241

Dr H. Harrison, Code RRE
Chief, Electrophysics Branch
National Aeronautics & Space Admin.
Washington, D.C. 20546

NASA Lewis Research Center
Attn: Library
21000 Brookpark Road
Cleveland, Ohio 44135

Los Alamos Scientific Laboratory
Attn: Report Library
P.O. Box 1663
Los Alamos, New Mexico 87544

Federal Aviation Administration
Attn: Admin Stds Div (MS-110)
800 Independence Ave S.W.
Washington, D.C. 20590

Head, Technical Services Division
Naval Investigative Service Headquarters
4420 North Fairfax Drive
Arlington, Virginia 22203

Commander
U.S. Naval Ordnance Laboratory
Attn: Librarian
White Oak, Maryland 21502 (2 copies)

Commanding Officer
Office of Naval Research Branch Office
Box 39 FPO
New York, New York 09510

Commanding Officer
Office of Naval Research Branch Office
219 South Dearborn Street
Chicago, Illinois 60604

Commanding Officer
Office of Naval Research Branch Office
495 Summer Street
Boston, Massachusetts 02210

Commander (ADL)
Naval Air Development Center
Johnsville, Warminster, Pa 18974

Commanding Officer
Naval Training Device Center
Orlando, Florida 32813

Commander (Code 753)
Naval Weapons Center
Attn: Technical Library
China Lake, California 93555

Commanding Officer
Naval Weapons Center
Corona Laboratories
Attn: Library
Corona, California 91720

Commander, U.S. Naval Missile Center
Point Mugu, California 93041

W.A. Eberspacher, Associate Head
Systems Integration Division
Code 5340A, Box 15
U.S. Naval Missile Center
Point Mugu, California 93041

Mr M. Zane Thornton, Chief
Network Engineering, Communications
and Operations Branch
Lister Hill National Center for
Biomedical Communications
8600 Rockville Pike
Bethesda, Maryland 20014

U.S. Post Office Department
Library - Room 1012
12th & Pennsylvania Ave, N.W.
Washington, D.C. 20260

Director
Research Laboratory of Electronics
Massachusetts Institute of Technology
Cambridge, Massachusetts 02139

Mr Jerome Fox, Research Coordinator
Polytechnic Institute of Brooklyn
55 Johnson Street
Brooklyn, New York 11201

Director
Columbia Radiation Laboratory
Columbia University
538 West 120th Street
New York, New York 10027

Director
Coordinated Science Laboratory
University of Illinois
Urbana, Illinois 61801

Director
Stanford Electronics Laboratories
Stanford University
Stanford, California 94305

Director
Microwave Physics Laboratory
Stanford University
Stanford, California 94305

Director, Electronics Research Laboratory
University of California
Berkeley, California 94720

Director
Electronic Sciences Laboratory
University of Southern California
Los Angeles, California 90007

Director
Electronics Research Center
The University of Texas at Austin
Austin Texas 78712

Division of Engineering and Applied Physics
210 Pierce Hall
Harvard University
Cambridge, Massachusetts 02138

Dr G.J. Murphy
The Technological Institute
Northwestern University
Evanston, Illinois 60201

Dr John C. Hancock, Head
School of Electrical Engineering
Purdue University
Lafayette, Indiana 47907

Dept of Electrical Engineering
Texas Technological College
Lubbock, Texas 79409

Aerospace Corporation
P.O. Box 95085
Los Angeles, California 90045
Attn: Library Acquisitions Group

Proffessor Nicholas George
California Inst of Technology
Pasadena, California 91109

Aeronautics Library
Graduat Aeronautical Laboratories
California Institute of Technology
1201 E. California Blvd
Pasadena, California 91109

The John Hopkins University
Applied Physics Laboratory
Attn: Document Librarian
8621 Georgia Avenue
Silver Spring, Maryland 20910

Raytheon Company
Attn: Librarian
Bedford, Massachusetts 01730

Raytheon Company
Research Division Library
28 Seyon Street
Waltham, Massachusetts 02154

Dr Sheldon J. Wells
Electronic Properties Information Center
Mail Station E-175
Hughes Aircraft Company
Culver City, California 90230

Dr Robert E. Fontana
Systems Research Laboratories Inc.
7001 Indian Ripple Road
Dayton, Ohio 45440

Nuclear Instrumentation Group
Bldg 29, Room 101
Lawrence Radiation Laboratory
University of California
Berkeley, California 94720

Sylvania Electronic Systems
Applied Research Laboratory
Attn: Documents Librarian
40 Sylvan Road
Waltham, Massachusetts 02154

Hollander Associates
P.O. Box 2276
Fullerton, California 92633

Illinois Institute of Technology
Dept of Electrical Engineering
Chicago, Illinois 60616

The University of Arizona
Dept of Electrical Engineering
Tucson, Arizona 85721

Utah State University
Dept Of Electrical Engineering
Logan, Utah 84321

Case Institute of Technology
Engineering Division
University Circle
Cleveland, Ohio 44106

Hunt Library
Carnegie-Mellon University
Schenley Park
Pittsburgh, Pennsylvania 15213

Dr Leo Youns
Stanford Research Institute
Menlo Park, California 94025

School of Engineering Sciences
Arizona State University
Tempe, Arizona 85281

Engineering & Mathmatical Sciences Library
University of California at Los Angeles
405 Hilgred Avenue
Los Angeles, California 90024

The Library
Government Publications Section
University of California
Santa Barbara, California 93106

Carnegie Institute of Technology
Electrical Engineering Department
Pittsburgh, Pennsylvania 15213

Professor Joseph E. Rowe
Chairman, Dept of Electrical Engineering
The University of Michigan
Ann Arbor, Michigan 48104

New York University
College of Engineering
New York, New York 10019

Syracuse University
Dept of Electrical Engineering
Syracuse, New York 13210

ERRATUM

Mr Jerome Fox, Research Coordinator
Polytechnic Institute of Brroklyn
55 Johnson St (Should be 333 Jay St)
Brooklyn, N.Y. 11201

OMIT

Mr Morton M. Pavane, Chief
AFSC Scientific & Tech. Liaison Office
26 Federal Plaza, Suite 1313
New York, New York 10007

Yale University
Engineering Department
New Haven, Connecticut 06520

Airborne Instruments Laboratory
Deerpark, New York 11729

Raytheon Company
Attn: Librarian
Bedford, Massachusetts 01730

Lincoln Laboratory
Massachusetts Institute of Technology
Lexington, Massachusetts 02173

The University of Iowa
The University Libraries
Iowa City, Iowa 52240

Lenkurt Electric Co,Inc
1105 County Road
San Carlos, California 94070
Attn: Mr E.K. Peterson

Philco Ford Corporation
Communications & Electronics Div.
Union Meeting and Jolly Rods
Blue Bell, Pennsylvania 19422

Union Carbide Corporation
Electronic Division
P.O. Box 1209
Mountain View, California 94041

Electromagnetic Compatibility Analysis Center
(ECAC), Attn: ACLP
North Severn
Annapolis, Maryland 21402

Director
U. S. Army Advanced Materiel Concepts Agency
Washington, D.C. 20315

ADDENDUM

Dept of Electrical Engineering
Rice University
Houston, Texas 77001

Research Laboratories for the Eng. Sc.
School of Engineering & Applied Science
University of Virginia
Charlottesville, Virginia 22903

Dept of Electrical Engineering
College of Engineering & Technology
Ohio University
Athens, Ohio 45701

Project Mac
Document Room
Massachusetts Institute of Technology
545 Technology Square
Cambridge, Massachusetts 02139

Lehigh University
Dept of Electrical Engineering
Bethelem, Pennsylvania 18015

Commander Test Command (TCDT-)
Defense Atomic Support Agency
Sandia Base
Albuquerque, New Mexico 87115

Materials Center Reading Room 13-2137
Massachusetts Institute of Technology
Cambridge, Massachusetts 02139

Professor James A. Cadzow
Department of Electrical Engineering
State University of New York at Buffalo
Buffalo, New York 14214

Security Classification

DOCUMENT CONTROL DATA - R & D

(Security classification of title, body of abstract and indexing annotation must be entered when the overall report is classified)

1. ORIGINATING ACTIVITY *(Corporate author)* University of Illinois Coordinated Science Laboratory Urbana, Illinois 61801	2a. REPORT SECURITY CLASSIFICATION Unclassified 2b. GROUP

3. REPORT TITLE

TUNNELING IN SEMICONDUCTORS

4. DESCRIPTIVE NOTES *(Type of report and inclusive dates)*

5. AUTHOR(S) *(First name, middle initial, last name)*

DUKE, C. B.

6. REPORT DATE	7a. TOTAL NO. OF PAGES	7b. NO. OF REFS
August, 1969	24	43

8a. CONTRACT OR GRANT NO. DAAB 07-67-C-0199; also in part JPL b. PROJECT NO. 952383	9a. ORIGINATOR'S REPORT NUMBER(S) R-425
c. d.	9b. OTHER REPORT NO(S) *(Any other numbers that may be assigned this report)*

10. DISTRIBUTION STATEMENT

This document has been approved for public release and sale; its distribution is unlimited.

11. SUPPLEMENTARY NOTES	12. SPONSORING MILITARY ACTIVITY Joint Services Electronics Program thru U.S. Army Electronics Command Fort Monmouth, New Jersey 07703

13. ABSTRACT

Historical highlights of studies of current flow across metal-semiconductor contacts via electron tunneling are outlined. The physical origin of the space-charge potential at a rectifying metal contact on a degenerate semiconductor is illustrated with emphasis on the features of this potential which determine the dominant mechanism of current flow across the contact. Recent experiments on the tunneling characteristics of those junctions are described. Their interpretation in terms of phenomenological independent-electron models is discussed critically. The tunneling spectroscopy of collective excitations is described by use of the transfer-Hamiltonian model. The influence of features of the phonon spectra in the semiconductor on inelastic tunneling is illustrated for Ge. The effects of electronic interactions with collective excitations in the semiconductor electrode are discussed for phonons in Si and CdS, and for plasmons in GaAs. The references given herein supplement those presented in a recent comprehensive review.

DD FORM 1 NOV 65 1473

Security Classification

Security Classification

14 KEY WORDS	LINK A		LINK B		LINK C	
	ROLE	WT	ROLE	WT	ROLE	WT
Tunneling						
Semiconductor						
Metal Semiconductor Contact						

Security Classification